

# Analytical Methods

Accepted Manuscript



This is an *Accepted Manuscript*, which has been through the Royal Society of Chemistry peer review process and has been accepted for publication.

*Accepted Manuscripts* are published online shortly after acceptance, before technical editing, formatting and proof reading. Using this free service, authors can make their results available to the community, in citable form, before we publish the edited article. We will replace this *Accepted Manuscript* with the edited and formatted *Advance Article* as soon as it is available.

You can find more information about *Accepted Manuscripts* in the [Information for Authors](#).

Please note that technical editing may introduce minor changes to the text and/or graphics, which may alter content. The journal's standard [Terms & Conditions](#) and the [Ethical guidelines](#) still apply. In no event shall the Royal Society of Chemistry be held responsible for any errors or omissions in this *Accepted Manuscript* or any consequences arising from the use of any information it contains.

1  
2  
3  
4 1 **Non-destructive gender identification of silkworm cocoon using x-ray imaging**  
5  
6 2 **technology coupled with multivariate data analysis**

7  
8  
9 3 **Running title: *Gender Identification of Silkworm Cocoon with X-ray Imaging***

10 4 Jian-rong Cai\*, Lei-ming Yuan, Bin Liu and Li Sun  
11 5 School of Food & Biological Engineering, Jiangsu University, Xuefu Road 301, Zhenjiang City,  
12 6 Jiangsu Province, 212013, China.

13 7 \*Corresponding author: Jian-rong Cai, e-mail: jrcai@ujs.edu.cn.  
14 8

15  
16  
17 9 **Abstract**

18  
19 10 A rapid, reliable and non-destructive method for gender discrimination of  
20 11 silkworm cocoon is of great importance to the mulberry silkworm industry for  
21 12 producing high quality silk. The objective of this study was to determine the  
22 13 feasibility of soft X-ray imaging with multivariate data analysis to classify the gender  
23 14 of silkworm cocoon. X-ray images of silkworm cocoon were obtained and  
24 15 pre-processed, and then region of interest (ROI) of chrysalis was segmented. Totally  
25 16 11 morphological characters of chrysalis were extracted and compressed by principal  
26 17 component analysis (PCA) to visualize the cluster trends. In developing the  
27 18 discrimination classifiers, four kinds of algorithms including K-nearest neighbors  
28 19 (KNN), linear discriminant analysis (LDA), back propagation artificial neural network  
29 20 (BP-ANN) and support vector machine (SVM) were comparatively employed, and the  
30 21 performance of those models were optimized by cross validation. The results  
31 22 indicated that the correct identification rates of these classifiers were all high and in  
32 23 the range from 92.57% obtained via SVM to 93.68% obtained via KNN. On the  
33 24 consideration of the running time, LDA classifier was highlighted for its 93.31%  
34 25 accuracy. The results indicated this X-ray imaging technique with multivariate  
35 26 analysis could successfully be used in the screening of the gender of silkworm cocoon  
36 27 in the mulberry silkworm industry.

37  
38  
39 28 **Key words:** *X-ray imaging technique; silkworm cocoon; pattern recognition; image*  
40 29 *process; gender identification*  
41 30

42  
43  
44  
45  
46  
47  
48  
49  
50  
51  
52  
53 31 **1. Introduction**

54  
55 32 Silkworm silk is one of the most important materials utilized extensively in the  
56 33 textile industry. Undoubtedly, the silkworm silk with high quality draws consumers'  
57 34 purchasing tendency and gains a bigger market share. The mulberry silkworm & silk

1  
2  
3 35 industry is a traditional industry in China, and the exportation of silk is going to  
4 36 increase every year. There are gender differences in mulberry silkworm industry, and  
5 37 the silk of male silkworm has advantages over the female silkworm, and its price is  
6 38 higher. According to experience, the silkworm silk produced by male silkworm  
7 39 basically has several advantages such as more even fineness, higher grade of raw silk,  
8 40 and better elasticity. Thus silkworm cocoons are usually separated according to their  
9 41 genders manually. This can greatly improve the quality of silk products without  
10 42 increasing any inputs.

11 43 At the present stage, the mostly used method is that cutting the cocoon by  
12 44 manual operation and identifying the pupa gender by its physical features. This  
13 45 traditional method seems to be less effective when large amount of silkworms need to  
14 46 be classified at the breeding season or before the reeling process because of  
15 47 consuming mass labor. Moreover it is likely to damage the pupa and judge falsely,  
16 48 which causes the male and female pupa mixed. The mix up of pupas brings about  
17 49 parental pupa copulations, which will weaken the quality of silkworm eggs. Thus, it is  
18 50 of great importance to separate the female from the male, and to exert the advantages  
19 51 of male silkworm cocoon. In this situation, a rapid, reliable and nondestructive  
20 52 method, which can reduce manpower, accelerate identification and be limited damage  
21 53 to pupas, is urgently required for discriminating the gender of silkworm cocoon.

22 54 Near infrared spectroscopy (NIRS) is an all-purpose analysis method, and its  
23 55 excellent analysis has been proved in agriculture products<sup>1,2</sup>. The attempt of  
24 56 reflectance spectra of pupas with chemo-metrics has been used to inspect gender of  
25 57 silkworm and obtained more than 90% identification rates for gender discrimination<sup>3</sup>.  
26 58 However, some pre-processes were needed before NIRS approaching, such as cocoon  
27 59 cutting, fixed point of spectral reading, et al. What's more, the accuracy of NIR  
28 60 determination was affected by temperature, humidity, the distance between detector  
29 61 and acquiring point.

30 62 Other promising non-destructive approaches can be investigated via the  
31 63 differences of morphological characters according to the gender of silkworm cocoon.  
32 64 With the image processing technique, shape representation and description techniques  
33 65 can be developed to distinguish the gender of silkworm cocoon. Thus the projective  
34 66 information of silkworm chrysalis is possible to study the discrimination. With the  
35 67 illumination of a UVA light source, female silkworm pupa can be distinguished from  
36 68 the male via fluorescent imaging technique<sup>4</sup>. But this technique is limited to some  
37 69 species because of the improvement of silkworms through dye-modified diet and

1  
2  
3 70 cross breeding <sup>5</sup>. Magnetic resonance imaging (MRI) technology was employed to  
4 71 capture the weighted images and was considered as a potential technique to classify  
5 72 the silkworm genders <sup>6</sup>, but with key disadvantages on the speed and the equipment  
6 73 cost. In order to settle above problems, a few low-cost light emitting diodes (LED)  
7 74 were proposed and demonstrated on silkworm pupa <sup>7</sup>. Each LED emitted different  
8 75 wavelength spectra on pupa, and special characterizers only found on female chrysalis  
9 76 <sup>8</sup>. This optical penetration-based silkworm pupa gender identification was studied and  
10 77 88% discrimination accuracy was obtained <sup>9</sup>. Obviously, the identification rates of  
11 78 those attempts based on the computer vision were not better than the result of NIRS  
12 79 approach. But the exercisable ability of computer vision in identifying the gender of  
13 80 silkworm pupas let it highlight from other approaches, such as NIRS <sup>3</sup>, weighting <sup>10</sup>,  
14 81 MRI <sup>6</sup>, DNA analysis <sup>11</sup> et al.. However, a key problem that exists in the application  
15 82 of computer vision is that the cocoon must be cut before capturing the projective  
16 83 information, which will tremendously weaken the practical utilization.

17 84 X-ray, also called roentgen ray, is a type of electromagnetic radiation with the  
18 85 wavelength 0.01~ 10 nm. The energy of photon in X-ray system usually is higher than  
19 86 100 keV, which results a strong penetrability to the target objects. The wavelength in  
20 87 range 1~10 nm is often called as soft X-ray, whose applications were arisen in food  
21 88 inspection. The principle of soft X-ray inspection is on the basis of density of product  
22 89 and the contaminant. X-ray is one of the most effective tool to inspect the agriculture  
23 90 products, such as the inside defects of pecan <sup>12</sup>, fungal infection in wheat <sup>13</sup>, the  
24 91 defrosted fruit <sup>14</sup>.

25 92 Due to the differences in the density of cocoon and chrysalis, X-ray image of  
26 93 silkworm cocoon can exhibit the discrepant information: penetration intensity in  
27 94 cocoon area is higher than that in chrysalis area. These discrepant representations can  
28 95 be described by image process <sup>15</sup> and are used as the input of supervised classifiers,  
29 96 which are calibrated by pattern recognition methods. Therefore, in this study an  
30 97 appropriate X-ray imaging technique coupled with image process, pattern recognition  
31 98 methods was proposed. The objective of this study was to determine the potential of  
32 99 soft X-ray imaging with multivariate data analysis to classify the gender of silkworm  
33 100 cocoon in the mulberry silkworm industry.

## 34 101 **2. Materials and methods**

### 35 102 **2.1 Samples Collection**

36 103 Three hybrid varieties of silkworm samples (*Bombyx mori* L.) were collected for  
37 104 this experiment, and all samples were provided by Zhenjiang Sericulture Research

1  
2  
3 105 Institute, Chinese Academy of Agricultural Sciences. The hybrid varieties were  
4 106 'JingSong'×'HaoYue', 'Shuangkang'×'Yongkang' and 'Suzhen'×'Chunguang'  
5  
6 107 respectively. Couples of batches of samples were gathered from two seasons 2009.06  
7  
8 108 and 2010.06. Each batch of about 80~100 samples was carried to the laboratory for at  
9  
10 109 least 12 hours storage before X-ray imaging operation. Once finishing the X-ray scan,  
11 110 the samples were delivered to Sericulture Research Institute and the gender was  
12 111 checked by the traditional approach. The technologist cut the cocoon and identified  
13 112 the gender by the inherent morphological features of pupa. In the routine of  
14 113 identifying the gender of silkworm pupas, some unqualified samples were got rid of,  
15 114 such as rotten or dead chrysalis. **Fig.1** shows the photograph information of silkworm  
16 115 cocoon and silkworm pupa.

## 116 2.2 X-ray Imaging Acquisition

117 In this experiment, a soft X-ray digital imaging system (**Fig.2**) was utilized,  
118 which consisted of a frame grabber, X-ray controller, detector, tube, stepper motor,  
119 conveyor belt, protective cover and computer, along with appropriated software  
120 (X-view4.2). The wave, which generated by the X-ray tube (model: *T80-1-60*,  
121 voltage: 20kV~160kV, current: 0.1mA~1mA, *Beijing mechanical and electrical*  
122 *technology company, China*), penetrated through the detected sample on the conveyor  
123 belt and was captured by X-ray detector (model: *0.4f2-307*, line scanning 1\*768, pixel  
124 size: 0.4mm, scanning speed: 0.1~0.8m/s, *DT company, Finland*). Then the incoming  
125 wave of X-ray detector was first converted to visible light and accurately measured.  
126 After signal processing by X-ray detector, the digital data signal was sent to the frame  
127 grabber. During samples moving on conveyor belt, sequential signals were acquired  
128 by this linear scan frame grabber. At last an image (1024\*768 pixel size) featured  
129 with gray information was manually obtained and then displayed on computer screen.

130 Before grabbing the radiographs of silkworm cocoon, some parameters of the  
131 X-ray system were optimized by preliminary works, and those parameters were: a) the  
132 speed of conveyer belt was set to 0.15m/s; b) the integration time of X-ray detector  
133 was set to 2.22ms; c) the voltage of X-ray tube was set to 40kV; d) the current was set  
134 to 0.6mA. The X-ray detector was calibrated as the literature <sup>16</sup> described to eliminate  
135 the differences in six modules of X-ray detector. The cocoon and pupa could be both  
136 penetrated through by X-ray energy. What's more, the differentiation in penetration  
137 through cocoon and pupa was different due to their density properties. Thus image  
138 part of pupa region was darkened and highlighted from cocoon or belt. After setting  
139 the imaging parameters and calibrating X-ray detector, several samples were put

140 simultaneously without any touch or overlap to each other on the conveyer belt and  
 141 grabbed radiographs by this soft X-ray digital imaging system. Images were acquired  
 142 with silkworm cocoons in a random orientation and were read in 12-bit resolution.

### 143 **2.3 Image processing and features extraction**

144 A full depiction of the key steps involved in image processing algorithms for  
 145 identifying the gender of silkworm cocoons is shown in a flow chart presented in  
 146 **Fig.3**. The algorithm had various steps of process. The first step was for image  
 147 pre-processing and segmentation. The second step was for geometrical feature  
 148 extraction, such as area, perimeter, parameters of ellipse and shape. The third step was  
 149 to build a robust classification model for gender discrimination. The first two steps  
 150 were conducted in a portable computer with OpenCV1.0 (opening computer vision  
 151 library, version 1.0) and VC++6.0, and the third step was investigated in Matlab  
 152 (version 2008a, the Mathworks, USA) to obtain an appropriate classifier.

#### 153 **2.3.1 Image pre-processing and segmentation**

154 **Fig.4** shows the binary image of the silkworm cocoon after being processed, and  
 155 some differences can be seen between pupas. **Fig.5a** shows the original X-ray image,  
 156 where the region of the pupa is darker than others. Before image segmentation, grey  
 157 contrast enhancement and de-noising filter were employed to enhance the region of  
 158 pupa part. And after segmentation, morphological operations were needed to filter out  
 159 the unwanted regions (i.e. noises).

160 Firstly, in the aspect of grey contrast enhancement, the grey value of pixel was  
 161 stretched as **Eq.1** described. The value lower than 150 in  $f(x,y)$  was set to 0 and that  
 162 higher than 250 was set to 255, while the value in the interval [150, 250] was  
 163 stretched to [0, 255].

$$164 \quad f'(i, j) = \begin{cases} 0, & 0 \leq f(i, j) < 150 \\ \frac{255-0}{250-150} \times [f(i, j) - 150], & 150 \leq f(i, j) \leq 250 \\ 255, & 250 < f(i, j) \leq 255 \end{cases} \quad \text{Eq.1}$$

165 Where  $f(x,y)$  is the grey value in original image **Fig.5a**, and  $f'(x,y)$  is the stretched  
 166 grey value **Fig.5b**.

167 Then, de-noising filter was tried to remove the noise, which might be solid  
 168 particle, cocoon or other sundries. A Gaussian filter of  $3 \times 3$  window size was used to  
 169 remove those noises and the result was better than average, median, and wiener filters  
 170 on the enhanced image. A Gaussian filter is a line filtering technique which allows the

171 edges to be preserved while filtering out the unwanted noise. It replaces the original  
172 pixel with the Gaussian of its 8-neighbouring pixel values. **Fig.5c** shows the  
173 de-noising image, and the edge of pupa region can be clear from the background (i.e.  
174 the conveyor belt and the cocoon).

175 Next, a global threshold segmentation method as **Eq.2** shown was utilized to  
176 separate the silkworm pupa from the background. The grey value of pixels which was  
177 lower than 250, was set to 0, and grey value of the rest pixels was set to 1. The result  
178 of the threshold image was a discrete binary image, which as **Fig.5d** shown, mixed  
179 with some small regions, which needed to remove.

$$180 \quad g(i,j) = \begin{cases} 0, & f'(i,j) < 250 \\ 1, & f'(i,j) \geq 250 \end{cases} \quad \text{Eq.2}$$

181 Where  $f'(x,y)$  is the filtered image **Fig.5c**, and  $g(x,y)$  is the binary image **Fig.5d**  
182 (**Fig.4** is a result of the above process).

183 Finally, a morphological operation was utilized in order to reduce or eliminate the  
184 unwanted regions (undesired speckles outside of the pupa). Opening operation of  $3 \times 3$   
185 window size was highlighted over erosion or dilation on the performance of the  
186 segmented output as **Fig.5e** shown, small regions of noises were removed and only  
187 the region of pupa was remained.

### 188 **2.3.2 Features extraction**

189 A simple trick was needed to check whether the outputs were the region of  
190 interest (ROI) for silkworm chrysalis. Firstly outputs were sorted by their columns or  
191 rows and each region was read one by one according to its sequence. Then two  
192 parameters (i.e. *Area* and *Perimeter*) were extracted from this output region to  
193 validate whether it was the ROI for pupae by the discriminated criteria: a) area >1000;  
194 b) perimeter >120. If one of region's parameters could not meet the designed criteria,  
195 the output would be ignored and returned to a next region. Only the extracted  
196 parameters of output regions met the both two conditions, the output should be  
197 acknowledged as ROI for pupa region. An object can be represented in features of its  
198 external characteristics, and there are many features can be used to describe an object.  
199 Thus, usually the objects of one class can be distinguished from the others by their  
200 shapes, which are physical dimensional measurements that characterize the  
201 appearance of an object. According to the geometrical differences between male and  
202 female pupa, several invariant features about size and shape of the ROI were extracted  
203 orderly as depicted in the literature<sup>15</sup>.

1  
2  
3 204 The descriptors of ellipse about major axis ( $R_a$ ), minor axis ( $R_b$ ), and the Ratio  
4 205 ( $R_a/R_b$ ), and the descriptors of shape about eccentricity, roundness, rectangularity,  
5 206 and complexity were calculated. Additionally, the rested shape features  $S1$  and  $S2$ ,  
6 207 which used to describe the concave-convex of region, were counted by **Eq.3**.

9  
10  
11 208 
$$\begin{cases} S1 = Area / S_c \\ S2 = Area / S_r \end{cases} \quad \text{Eq.3}$$
  
12  
13

14 209 Where  $Area$  is the area of the ROI, and  $S_c$  is the area of external minimum convex  
15 210 polygon, and  $S_r$  is the area of minimum enclosing rectangle.

## 18 211 **2.4 Multivariate Data Analysis**

19  
20 212 The Matlab software was used for data treatment with ChemAC toolbox and  
21 213 libsvm toolbox on portable computer (ASUS, Inter core i2, CPU6670@2.2GHz).

### 23 214 **2.4.1 Principle component analysis**

24  
25 215 Mass original data can be transformed to a few new variables, usually called PC  
26 216 (principal component, PC) by principal component analysis (PCA), which is a data  
27 217 reconstruction and dimensional reduction method. Each PC is the linear combination  
28 218 from the input variables, and as a vector is orthogonal simultaneously to the rest. PCs  
29 219 are arranged in the order of eigenvalues from large to small. Usually, the first few PCs  
30 220 can account for the greatest proportion of the original information. Also, PCA is an  
31 221 unsupervised pattern recognition method which is used for visualizing samples trends  
32 222 in a limited dimensional space. Thus, the plot of some top PCs can be used to handily  
33 223 examine the distance between different classes. Prior to perform PCA, the feature  
34 224 matrix is normalized to the range of 0~1, which can be eliminated the numerical  
35 225 difference of the features (e.g. usually  $Area > 1000$ , while  $R_b < 40$ ). In this work, PCA  
36 226 was performed on all variables, and some of the top PCs were employed as the input  
37 227 of classifiers.

### 40 228 **2.4.2 Pattern recognition methods**

41 229 Supervised classifiers of linear discriminant analysis (LDA), K nearest neighbors  
42 230 (KNN), back propagation artificial neural network (BP-ANN) and support vector  
43 231 machine (SVM), were employed in this research in order to discriminate the gender of  
44 232 silkworm cocoon.

45  
46  
47  
48  
49  
50  
51  
52  
53  
54  
55 233 According to the principle of supervised pattern recognition, all collected samples  
56 234 were divided into two subsets: calibration set and prediction set. The samples in  
57 235 calibration set used to develop the classifiers, while the samples in prediction set used

236 to test the performance of the developed classifiers. Correct identification rate (CR) is  
237 commonly used to appraise the performance of the classifiers on correctly predicting  
238 the sample's category of the prediction set. The higher the CR is, the better the  
239 classifier has the ability of predicting unknown samples.

240 Besides, the average prediction time of samples by the classifiers was taken into  
241 account. The prediction time can be accounted for the discrimination model's  
242 complexity to some extent. With the satisfied prediction, the less the time is  
243 consumed, the simpler the classifier is better, which will add the applicability of the  
244 model to the practice and can be suitable for fast determination.

### 245 **3 Results and Discussion**

#### 246 **3.1 Samples Statistics**

247 As **table 1** shown, totally about 1071 samples were collected for this experiment.

248 These samples came from two seasons and varied in three hybrid varieties. The  
249 gender ratio of all samples was close to 1:1, which was similar to Pan's study<sup>3</sup>.

250 Samples from 'JingSong'×'HaoYue' variety were gathered sub-totally 294 (27.45%  
251 of all) in 2009.06 and 603 (56.3% of all) in 2010.06, respectively. Another two  
252 varieties, 'Shuangkang'×'Yongkang' 86 samples and 'Suzhen'×'Chunguang' 88  
253 samples, were both brought in 2010.06, and had 8.03 and 8.22 percentage of all  
254 repetitively. Diversity of samples in this research can expand the generalization of the  
255 developed classifiers. **Table 2** shows the statistical result of morphological features of  
256 silkworm. Those features were extracted from X-ray image after a series of image  
257 process operations. The *Area* of ROI (i.e. region pixel of pupa in X-ray image) has the  
258 biggest coefficient of variable among all descriptors. This illustrated the projective  
259 area of pupa was in a broad range of parameter *Area*. Largish distribution differences  
260 of other features (i.e. *Perimeter*, *Ra*, *Rb*, *Ra/Rb*, *S2*) also indicated diversities of  
261 morphological features in silkworm pupas.

262 There was a dataset by matrix sizes of 1071 rows×12 columns (i.e. 11 features  
263 and 1 gender in column). Dataset was divided into calibration set and prediction set,  
264 respectively. The ratio between the number of calibration set and prediction set was  
265 set to 3:1. As a result, totally 802 samples were included in calibration set, and 269  
266 samples were included in prediction set. At the aspect of dividing, each sample was

267 randomly divided into calibration or prediction set according to its arrival batch or  
268 variety. Detail of the dividing result is shown in **table 3**.

### 269 **3.2 PCA performance**

270 One object has many descriptors about its shape, region, contour, etc., and those  
271 descriptors have their inner relationships. Consequently, these morphological  
272 characterizers of pupa contain overlapped information (i.e. redundant information) for  
273 one sample<sup>17</sup>. In this experiment, all features (i.e. 11 variables) extracted from X-ray  
274 images were used for the PCA. Albeit PCA is not a supervised classifier tool, its  
275 properties could provide morphological information trends as a result of the gender  
276 difference of silkworm. In order to visualize the cluster trends of these samples, a 2D  
277 score scatter plot was figured with employing the top two PCs (i.e. PC1 and PC2) of  
278 the calibration set samples as shown in **Fig.6**. The labels of “Female” and “Male”  
279 were attached to samples according to their actual genders. PC1 explained 39.59%  
280 variance (i.e. got 39.59% information from 11 raw variables), and PC2 also explained  
281 32.9% variance. A total of top two PCs captured accumulatively 72.49% variability of  
282 original information. In this 2D scatter plot, most samples clustered well along the  
283 axis plane. It was apparent that there was a separation between the gender clusters  
284 which indicated possibly to be separated, as well as a transition region (i.e clusters  
285 overlapped) which indicated a slight similarity of morphological features between  
286 genders. This overlapped part could be attributed partly to the projection imaging of  
287 randomly placing pupas. The goal of this work was to classify the gender of silkworm  
288 by means of X-ray imaging approach with the help of the supervised pattern  
289 recognition methods. Therefore, it was crucial to choose a suitable pattern recognition  
290 method for developing a classifier.

### 291 **3.3 Results of pattern recognition methods**

292 The geometrical exploration of above 2-D plot by PCA only gives the data cluster  
293 trend. Therefore, it is a key step to choose the suitable classification tool. In this work,  
294 four linear or nonlinear classification tools (i.e. LDA, KNN, BP-ANN, and SVM)  
295 were attempted to develop the discrimination models (i.e. classifiers). These  
296 classifiers were optimized by cross validation. The group sets of cross validation came  
297 from the five-equal segments in calibration set when developing these discrimination  
298 models.

### 3.3.1 LDA result

LDA is the most commonly used algorithm among the supervised pattern recognition methods. LDA is considered to find the linear combination of inputs and the resulting combination that may separate two or more categories of events or objects. It maximizes the ratio of between-class variance to the within-class variance in any particular data set thereby guaranteeing maximal separability. It has been successfully utilized in cocoa beans<sup>18</sup>, vinegar acetic fermentation<sup>19</sup>, and tea varieties<sup>20</sup>. It is crucial that the appropriate number of PCs will enhance the performance of LDA classifier. Frequently, LDA model is optimized to select the appropriate number of PCs by means of cross-validation in developing this discrimination model. The optimal quantity of PCs was specialized according to the highest identification rates by cross-validation. Then the back identification rate was made for calibration and prediction set as **Fig.7** shown according to the consecutive PCs. As shown in **Fig.7**, increasing by the quantity of PCs, the CR for prediction set firstly trended from the low 79.93% to the high 93.31% and then remained unchanged at 92.94%. Obviously, the best LDA classifier was obtained when the top two PCs were utilized, and the correct identification rates were 93.52% and 93.31% in the calibration and prediction sets, respectively. **Table 3** shows the details of LDA classifier with top two PCs for calibration set and prediction set.

### 3.3.2 KNN result

KNN has been developed to be a powerful method of classification and has proved to be utilized successfully in many applications such as tea grade<sup>21</sup>, pork storage time<sup>22</sup>, et al.. It is a machine learning technique on the basis of linear supervised pattern recognition. An unknown sample in prediction set is classified depending on the majority of its  $K$  nearest neighbors (i.e. samples) in calibration set. Thereby parameter  $K$  greatly influences on the identification rate of KNN classifier. Generally the prediction accuracy for a given set of  $K$  values are estimated by cross-validation, and the value of parameter  $K$  that gives the maximum discrimination accuracy (i.e. lowest discrimination error) is selected by cross-validation. In this study, the quantity of PCs (PCs=2, 3, ..., 11) and  $K$  values ( $K=1, 3, 5, 7, 9$ ) were optimized simultaneously by cross-validation. According to the quantity of PCs and the  $K$  values, the developing KNN model was tested by the prediction set, and **Fig. 8** shows the correct discrimination rates. The same as the number of PCs affected the performance of KNN model, it was found that the value of parameter  $K$  influenced the

333 discrimination accuracy as well. The best KNN classifier was achieved when  $K=3$  and  
334 PCs=2, and the discrimination accuracy was 93.68% for prediction set.

### 335 3.3.3 BP-ANN result

336 In consideration of which the linear model may fail to provide a complete  
337 solution to the classification problem, some non-linear approaches such as artificial  
338 neural network (ANN) and support vector machine (SVM) were used in this study. As  
339 a classification algorithm ANN is well known, and some literatures have reported its  
340 applications in solutions to classification problem of agricultural products<sup>23</sup>. There  
341 are many types of ANN, and each type may perform well in a certain instance. Here a  
342 type of ANN called back propagation artificial neural network (BP-ANN) was  
343 adopted. In the routine of developing BP-ANN classifier, many parameters exerted to  
344 some extent to certainly influence on the performance of the conclusive model. These  
345 parameters were: the number of neurons in the hidden layer, scale functions,  
346 momentum, initial weights and learning rate. In this study, the classical BP-ANN with  
347 three layers topology (i.e. Input Layer, Hidden Layer, and Output Layer) was  
348 constructed to calibrate a discrimination model<sup>23</sup>. The PCs ( $n=1,2,\dots,11$ ) were used  
349 as the Input Layer of BP-ANN model, and the gender (i.e. 0 = female, and 1 = male)  
350 was used as the Output Layer of BP-ANN model. In this work those parameters were  
351 optimized by cross validation on the basis of the calibration samples. In developing  
352 BP-ANN model, each model was calibrated at least 15 times. Finally, the parameter  
353 number of neurons in the Hidden layer was set to 5, and the parameter scale function  
354 was set to 'purelin', and the parameter learning rate was set to 0.1. Additionally, the  
355 result which was optimized by cross validation showed that some parameters were not  
356 the key and had hardly any impacts on the final classifier, such as initial weights and  
357 momentum. Besides, it was crucial to optimize the quantity of PCs in calibrating  
358 BP-ANN classifier. **Fig. 9** shows the correct identification rates by cross validation on  
359 the basis of the calibration samples according to the quantity of PCs. The optimal  
360 BP-ANN classifier was achieved when top four PCs (totally explained 94.74%  
361 variance) were included. The eventual BP-ANN classifier was structured with 4-5-1  
362 topology. The back identification rate was 94.44% for the calibration set, and the  
363 correct identification rate was 93.31% for the prediction set.

### 364 3.3.4 SVM result

365 Another non-linear classification tool, support vector machine (SVM) was  
366 employed in this study and attempted to obtain a better result. SVM was firstly

1  
2  
3 367 proposed by Vapnik and Chervone<sup>24</sup>, and further developed by Cortes and Vapnik<sup>25</sup>.  
4 368 It works by creating a hyper-plane between two different categories for classification.  
5 369 The aim of SVM specializes to find a hyper-plane that can be used to distinguish these  
6 370 data points between two categories. If two classes can not be enough separated by a  
7 371 linear boundary in the low dimension space, it is possible to transform this linear  
8 372 boundary to a hyper-plane which should allow linear separation in the higher  
9 373 dimension space. This transformation is implemented by a kernel function<sup>26</sup>, and  
10 374 usually three kernel functions are: polynomial, radial basis function (RBF), and  
11 375 sigmoid. As far as their computation, the structure of RBF is the fastest and simplest  
12 376 among those kernel functions. It is often a good choice to select RBF kernel function  
13 377 and resulting good performance of SVM. Therefore, only RBF kernel function was  
14 378 employed to undertake this transformation in this study.

15 379 When using RBF kernel function, there are two parameters are introduced, and  
16 380 they are penalty parameter  $C$  and kernel parameter  $\gamma$  respectively<sup>27</sup>. In this  
17 381 experiment, to obtain a good performance of SVM classifier, these two parameters  
18 382 were generally optimized by applying “grid search” to search the best combination ( $C$ ,  
19 383  $\gamma$ ). Basically pairs of ( $C$ ,  $\gamma$ ) were conducted and the resulting one with the best  
20 384 performance of SVM classifier by cross validation was collected. The grid  $\gamma=2^{-10}$ ,  
21 385  $2^{-9}$ , ...,  $2^9$ ,  $2^{10}$ , respectively, and  $C=2^{-10}$ ,  $2^{-9}$ , ...,  $2^9$ ,  $2^{10}$ , respectively, were attempted  
22 386 referring to Chen’ description<sup>21</sup>. Finally, this combination could be got from the  
23 387 contour map (**Fig.10a**), which showed a contour map for indicating various  
24 388 performances with different color. The optimal pair ( $C$ ,  $\gamma$ ) was achieved with  $\log_2(C)$   
25 389  $=2$ ,  $\log_2(\gamma)=1.4142$ , (i.e.  $C=4$ ,  $\gamma=2.665$ ), which was marked by a blue asterisk in the  
26 390 map. Certainly it was also crucial to optimize the number of PCs for developing SVM  
27 391 model by cross validation in calibration set. **Fig.10b** shows the correct identification  
28 392 rates by cross validation for both calibration and prediction set according to the  
29 393 quantity of PCs. The optimum SVM classifier was achieved when including top three  
30 394 PCs (totally explained 86.19% variance) and the back identification rate was 95.51%  
31 395 in the calibration set, and the predictive discrimination rate was 92.57% in the  
32 396 prediction set.

### 33 397 **3.3.5 Discussion of the Results**

34 398 In order to obtain a good performance in the classification of the gender of  
35 399 silkworm cocoon via X-ray imaging technique, pattern recognition methods and  
36 400 parameters optimization were conducted systematically in this work. **Table 4** shows  
37 401 the discrimination results of LDA, KNN, BP-ANN, and SVM classifiers. As seen

1  
2  
3 402 from this table, the linear models (i.e. LDA and KNN) achieved a little bit better  
4 403 results, as well as it employed a fewer PCs than the nonlinear classifiers (i.e. BP-ANN  
5 404 and SVM). The correct identification rates of the four classifiers were all higher than  
6 405 92%, and the result of KNN model was the best performance with 93.68% correct  
7 406 identification rate. At aspect of the averaged running time, LDA model cost the least  
8 407 time 3.3 milliseconds (ms) in predicting per sample, while the best KNN  
9 408 discrimination model needed 21.5 ms to finish the identification process. Considering  
10 409 that the practical utilization placed emphasis on the speed of determination, LDA  
11 410 model would be highlighted for its fast identification speed and the satisfying  
12 411 identification rate from the rests. Also as investigated from this table, we found that  
13 412 the correct identification rate for female samples was slightly higher than that for male  
14 413 samples except for SVM model. This would decrease the error discrimination of male  
15 414 silkworm, and thus benefit for the mulberry silkworm industry because of the male  
16 415 silkworm usually producing higher quality of silk than the female.

17 416 **Table 3** shows the details about the identification of LDA classifier for  
18 417 calibration set and prediction set. The correct identification rates for calibration or  
19 418 prediction samples collected in 2009.6 both were much lower than that collected in  
20 419 2010.6, what illustrated that there were morphological differences of pupas between  
21 420 seasons and the season factor affected much the robustness of the LDA classifier. But  
22 421 there was a just slight difference of the correct identification rates between three  
23 422 varieties from a same season. This indicated many similarities between varieties of  
24 423 silkworm, and the developed classifier based on one or more certain varieties could be  
25 424 used to predict the samples from other varieties. This correct identification rate was  
26 425 better than other study<sup>9</sup>. From above results, we could draw the conclusion that X-ray  
27 426 imaging technique coupled with pattern recognition methods had a great potential to  
28 427 identify the gender of silkworm cocoon. The following two aspects gave detailed  
29 428 discussions to this potential.

30 429 First of all, as seen from the operating principle of X-ray imaging system, the  
31 430 region of silkworm can be projected by X-ray energy penetration. Due to the low  
32 431 density of cocoon, the region of pupa is highlighted from the cocoon, and can be  
33 432 captured directly without cutting cocoon. With the help of image processing  
34 433 techniques, shape representations can be digitized and extracted effectively. Those  
35 434 representations are generally on behalf of the morphological characterizers of pupa.  
36 435 Thus, the X-ray imaging system has the ability to capture the physical information of  
37 436 silkworm directly without cutting cocoon, which is a great advantage over other

1  
2  
3 437 approaches<sup>3,8,9</sup>. However the representations' differences between the genders in  
4 438 morphological characterizers can not be easily identified by our naked eyes or  
5 439 experiences but with help of multivariate data analysis they can be differentiated  
6 440 effectively.

7  
8  
9 441 Secondly, as seen from the principles of multivariate data analysis methods, they  
10 442 act great roles in sexual identification of silkworm cocoon. PCA is used to eliminate  
11 443 the overlapped information and extract mainly useful information (i.e. PCs), and only  
12 444 top two PCs are involved in the final classifier. **Fig.11** shows the loadings of top two  
13 445 PCs against the 11 characteristic variables. A 2D scatter plot of variable-loadings for  
14 446 top two PCs is a good way to detect important variables since they represent the  
15 447 largest variations in the original information. Generally important variables have large  
16 448 absolute loadings value and are far way from origin point. The longer the distance  
17 449 between properties and coordinate origin point, the more the morphological property  
18 450 is important. As investigated from it, most of properties have contributed to the top  
19 451 two PCs, and each contributes much except one parameter *complexity*. However,  
20 452 limited information can be provided by PCA to estimate which property is important  
21 453 in developing a classifier, and this needs further explorations. Supervised pattern  
22 454 recognition methods have a strong capability of self-learning and self-adjusting, and  
23 455 can handle complex relationships between classes. Linear and nonlinear classifiers are  
24 456 employed comparatively to develop a robust classifier by optimizing parameters. Seen  
25 457 from the **table 4**, linear classifiers have included lower number of PCs, and got better  
26 458 performance than that of nonlinear classifiers. This is different to other studies where  
27 459 usually non-linear classifiers got better performances<sup>22</sup>. In some certain case the  
28 460 linear classifiers have a better capability of identifying the genders than nonlinear  
29 461 classifiers, as well as use a fewer number of PCs avoiding bringing noises to the  
30 462 classifiers. Moreover, it is of great importance to balance the model's performance  
31 463 and the running time when turning to the practical application. LDA classifier was  
32 464 considered as a desired discrimination model for its high correct identification rate  
33 465 and the least consuming time for predicting samples. Thus, with the help of LDA  
34 466 discrimination method, that the X-ray imaging system is proposed to identify the  
35 467 gender of silkworm made it possible.

#### 36 468 **4. Conclusion**

37 469 The overall results sufficiently demonstrated that the X-ray imaging technique  
38 470 with an appropriate classification tool could be successfully used to discriminate the  
39 471 gender of silkworm cocoon. After x-ray image processing, features extraction and

1  
2  
3 472 PCA reconstruction, four different linear and nonlinear classification tools (LDA,  
4 473 KNN, BP-ANN and SVM) were attempted comparatively to develop the  
5  
6 474 discrimination model in this research. Among these discrimination models, LDA  
7  
8 475 model achieved the optimum discrimination 93.31% with the least running time of  
9  
10 476 3.3ms. Compared with other discriminated methods such as NIRS, computer vision  
11  
12 477 based on visual light, and weighting, it can be concluded that X-ray imaging  
13  
14 478 technique coupled with classification tool shows its superiority in solution to classify  
15  
16 479 the gender of silkworm cocoon in the mulberry silkworm industry.

#### 16 480 **Acknowledgments**

17  
18 481 This work has been financially supported by the National Key Technology R&D  
19  
20 482 Program of China (Grant No. 2012BAD29B04-4) and the National Natural and  
21  
22 483 Science Foundation of China (30771243). Thanks to Zhenjiang Sericulture Research  
23  
24 484 Institute for their help in providing silkworm samples and identification of the gender  
25  
26 485 service. We are also grateful to many of our colleagues for stimulating discussion in  
27  
28 486 this field.

#### 28 487 **Compliance with Ethics Requirements**

29  
30 488 Jian-rong Cai, Lei-ming Yuan, Bin Liu, and Li Sun declares that there is no  
31  
32 489 conflict of interest. And this article does not contain any studies with human or animal  
33  
34 490 subjects.

#### 34 491 **Reference**

- 35  
36  
37 492 1. L.-M. Yuan, L. Sun, H. Lin, E. Han, H.-L. Liu and J.-R. Cai, *Spectrosc Spect*  
38  
39 493 *Anal*, 2013, **33**, 2387-2391.
- 40  
41 494 2. B. M. Nicolai, K. Beullens, E. Bobelyn, A. Peirs, W. Saeys, K. I. Theron and  
42  
43 495 J. Lammertyn, *Postharvest Biol Tec*, 2007, **46**, 99-118.
- 44  
45 496 3. S.-Y. Pan, M. Tao, A.-Q. Sun and T.-M. Jin, *Chinese Acta Entomologica*  
46  
47 497 *Sinica*, 1996, **39**, 360-365.
- 48  
49 498 4. H. Xiaolong, X. Renyu, C. Guangli, Z. Xing, Z. Yilin, Y. Xiaohua, Z. Yuqing  
50  
51 499 and G. Chengliang, *Molecular biology reports*, 2012, **39**, 1395-1409.
- 52  
53 500 5. N. C. Tansil, Y. Li, C. P. Teng, S. Zhang, K. Y. Win, X. Chen, X. Y. Liu and  
54  
55 501 M. Y. Han, *Advanced Materials*, 2011, **23**, 1463-1466.

- 1  
2  
3 502 6. C. Liu, Z. H. Ren, H. Z. Wang, P. Q. Yang and X. L. Zhang, Bmei 2008:  
4 Proceedings of the International Conference on Biomedical Engineering and  
5 503 Informatics, Vol 2, 2008.  
6  
7 504  
8  
9 505 7. S. Sumriddetchkajorn and C. Kamtongdee, *Appl Optics*, 2012, **51**, 408-412.  
10  
11 506 8. S. Sumriddetchkajorn, C. Kamtongdee and C. Sa-Ngiamsak, in *Sensing*  
12  
13 507 *Technologies for Biomaterial, Food, and Agriculture 2013*, 2013, vol. 8881.  
14  
15 508 9. C. Kamtongdee, S. Sumriddetchkajorn and C. Sa-ngiamsak, *Comput Electron*  
16  
17 509 *Agr*, 2013, **95**, 31-37.  
18  
19 510 10. M.-R. Babaei, H. Barari and K. Kara, *Pakistan Journal of Biological Sciences*,  
20  
21 511 2009, **12**, 443-446.  
22  
23 512 11. T. Fujii and T. Shimada, *Seminars in Cell & Developmental Biology*, 2007,  
24  
25 513 **18**, 379-388.  
26  
27 514 12. N. Kotwaliwale, P. R. Weckler, G. H. Brusewitz, G. A. Kranzler and N. O.  
28  
29 515 Maness, *Postharvest Biol Tec*, 2007, **45**, 372-380.  
30  
31 516 13. D. S. Narvankar, C. B. Singh, D. S. Jayas and N. D. G. White, *Biosyst Eng*,  
32  
33 517 2009, **103**, 49-56.  
34  
35 518 14. M. S. Nielsen, L. B. Christensen and R. Feidenhans'l, *Food Control*, 2014, **39**,  
36  
37 519 222-226.  
38  
39 520 15. C.-J. Du and D.-W. Sun, *Trends in Food Science & Technology*, 2004,  
40  
41 521 **15**, 230-249.  
42  
43 522 16. G.-P. Qu, Q. Ling, L.-Y. Guo, L.-H. Zhao and P.-J. Cheng, *Chinese Nuclear*  
44  
45 523 *Electronics & Detection Technology*, 2003, **23**, 414-416.  
46  
47 524 17. Q. Ouyang, J. Zhao and Q. Chen, *Food Res Int*, 2013, **51**, 633-640.  
48  
49 525 18. E. Teye, X. Huang, H. Dai and Q. Chen, *Spectrochimica Acta Part A:*  
50  
51 526 *Molecular and Biomolecular Spectroscopy*, 2013, **114**, 183-189.  
52  
53 527 19. Q. Chen, A. Liu, J. Zhao, Q. Ouyang, Z. Sun and L. Huang, *Sensors and*  
54  
55 528 *Actuators B: Chemical*, 2013, **183**, 608-616.  
56  
57 529 20. Q. Chen, J. Zhao and J. Cai, *T Asabe*, 2008, **51**, 623-628.  
58  
59 530 21. Q. Chen, J. Zhao, Z. Chen, H. Lin and D.-A. Zhao, *Sensors and Actuators B:*  
60  
531 *Chemical*, 2011, **159**, 294-300.

- 1  
2  
3 532 22. Q. Chen, J. Cai, X. Wan and J. Zhao, *LWT - Food Science and Technology*,  
4 2011, **44**, 2053-2058.  
5  
6  
7 534 23. C.-J. Du and D.-W. Sun, *Journal of Food Engineering*, 2006, **72**, 39-55.  
8  
9 535 24. V. N. Vapnik and A. Y. Chervonenkis, *Theory of Probability & Its*  
10 *Applications*, 1971, **16**, 264-280.  
11  
12 537 25. C. Cortes and V. Vapnik, *Machine learning*, 1995, **20**, 273-297.  
13  
14 538 26. U. Thissen, M. Pepers, B. Üstün, W. J. Melssen and L. M. C. Buydens,  
15 *Chemometr Intell Lab*, 2004, **73**, 169-179.  
16  
17  
18 540 27. S. S. Keerthi and C.-J. Lin, *Neural Computation*, 2003, **15**, 1667-1689.  
19  
20 541  
21  
22 542  
23  
24  
25  
26  
27  
28  
29  
30  
31  
32  
33  
34  
35  
36  
37  
38  
39  
40  
41  
42  
43  
44  
45  
46  
47  
48  
49  
50  
51  
52  
53  
54  
55  
56  
57  
58  
59  
60

543 **FIGURE CAPTIONS**

544

545 Figure 1 Picture of silkworm cocoon and silkworm pupa

546 Figure 2 Schematic of X-ray digital imaging system

547 Figure 3 Workflow of image processing and gender discrimination

548 Figure 4 The X-ray binary image of silkworm cocoons

549 Figure 5 The result of Image processes. (a) Original image; (b) Grey enhancement; (c)  
550 Gaussian filter; (d) Global threshold segmentation; (e) Opening operation output.

551 Figure 6 2-D scatter plot of the gender of silkworm cocoon. PC: principal component.

552 Figure 7 Correct identification rates of LDA model for calibration and prediction set  
553 according to different PCs.554 Figure 8 Correct identification rate of KNN classifier for prediction set according to  
555 different PCs and  $K$  values556 Figure 9 Correct identification rate of BP-ANN model for calibration and prediction  
557 set according to different PCs.558 Figure10 (a) Contour plot of the optimal parameter pairs  $(C, \gamma)$  by cross validation  
559 based on the calibration samples; (b) Correct Identification rates of SVM classifier  
560 with different PCs for calibration and prediction set.

561 Figure 11 The loadings of top two PCs against the 11 morphological variables

562

563 **Table 1** Statistical result of the sets of silkworm samples.

Experiment Time	Hybrid Varieties	Female Number	Male Number	Total (percentage)
2009.06	'JingSong'×'HaoYue'	150	144	294 (27.45%)
	'JingSong'×'HaoYue'	299	304	603 (56.3%)
2010.06	'Shuangkang'×'Yongkang'	37	49	86 (8.03%)
	'Suzhen'×'Chunguang'	45	43	88 (8.22%)
Total (percentage)		531 (49.58%)	540 (50.42%)	1071 (100%)

564

565

1  
2  
3  
4  
5  
6  
7  
8  
9  
10  
11  
12  
13  
14  
15  
16  
17  
18  
19  
20  
21  
22  
23  
24  
25  
26  
27  
28  
29  
30  
31  
32  
33  
34  
35  
36  
37  
38  
39  
40  
41  
42  
43  
44  
45  
46  
47  
48  
49  
50  
51  
52  
53  
54  
55  
56  
57  
58  
59  
60

566 **Table 2** Statistical results of the morphological features. SD: standard deviation; CV:  
567 coefficient of variable.

Features	Range	Mean	SD	CV(%)
<i>Area</i>	1051~2672	1897.1	243.2	12.82
<i>Perimeter</i>	139~225	186.5	12.205	6.54
<i>Ra</i>	56.7~91.9	76.43	5.013	6.56
<i>Rb</i>	23.4~38.7	31.7	2.324	7.33
<i>Ra/Rb</i>	1.88~2.80	2.42	0.129	5.33
<i>eccentricity</i>	0.85~0.93	0.91	0.011	1.21
<i>roundness</i>	0.61~0.76	0.68	0.023	3.38
<i>rectangularity</i>	0.73~0.78	0.78	0.003	0.38
<i>complexity</i>	16.6~20.6	18.4	0.623	3.39
<i>S1</i>	0.93~0.99	0.97	0.005	0.52
<i>S2</i>	0.51~0.86	0.74	0.057	7.70

568

569

570 **Table 3** Statistical results of LDA classifier for predicting calibration set and  
 571 prediction set. NFM: the number of actual female silkworms; NM: the number of  
 572 actual male silkworms; FM: female silkworm; M: male silkworm; CR: correct  
 573 identification rate.

Dataset	Season	Variety	Discriminated Gender				CR for	CR for	Total CR (%)
			NFM		NM		FM	M (%)	
			FM	M	FM	M	(%)		
Calibration (NFM= 400; NM=402)	2009-06	'JingSong'×'HaoYue'	103	8	14	95	88.03	92.23	90.00
		'JingSong'×'HaoYue'	206	19	8	219	96.26	92.02	94.03
	2010-06	'Shuangkang'×'Yongkang'	30	0	1	33	96.77	100.0	98.44
		'Suzhen'×'Chunguang'	34	0	2	30	94.44	100.0	96.97
		Count	373	27	25	377	93.72	92.32	93.52
Prediction (NFM= 131; NM=138)	2009-06	'JingSong'×'HaoYue'	35	4	6	29	85.37	87.88	86.49
		'JingSong'×'HaoYue'	69	5	2	75	97.18	93.75	95.36
	2010-06	'Shuangkang'×'Yongkang'	6	1	0	15	100.0	93.75	95.45
		'Suzhen'×'Chunguang'	11	0	0	11	100.0	100.0	100.0
		Count	121	10	8	130	93.80	92.86	93.31

574

575

1  
2  
3  
4  
5  
6  
7  
8  
9  
10  
11  
12  
13  
14  
15  
16  
17  
18  
19  
20  
21  
22  
23  
24  
25  
26  
27  
28  
29  
30  
31  
32  
33  
34  
35  
36  
37  
38  
39  
40  
41  
42  
43  
44  
45  
46  
47  
48  
49  
50  
51  
52  
53  
54  
55  
56  
57  
58  
59  
60

576 **Table 4** Statistical results of classifiers for predicting the gender of silkworm cocoon.  
577 LDA: linear discriminant analysis; KNN: *K* nearest neighbors, BP-ANN; back  
578 propagation artificial neural network; SVM: support vector machine; NFM: the  
579 number of actual female silkworms; NM: the number of actual male silkworms; FM:  
580 female silkworm; M: male silkworm. CR: correct identification rate.

Classifiers	Number of PCs	Discriminated Gender				CR for FM (%)	CR for M (%)	Total CR (%)	Running time (ms)
		NFM (131)		NM (138)					
		FM	M	FM	M				
LDA	2	121	10	8	130	93.80	92.86	93.31	3.3
KNN	2	120	11	6	132	95.24	92.31	93.68	21.5
BP-ANN	4	120	11	7	131	94.45	92.25	93.31	9.3
SVM	3	121	10	10	128	92.37	92.75	92.57	14.2

581

1  
2  
3  
4  
5  
6  
7  
8  
9  
10  
11  
12  
13  
14  
15  
16  
17  
18  
19  
20  
21  
22  
23  
24  
25  
26  
27  
28  
29  
30  
31  
32  
33  
34  
35  
36  
37  
38  
39  
40  
41  
42  
43  
44  
45  
46  
47  
48  
49  
50  
51  
52  
53  
54  
55  
56  
57  
58  
59  
60

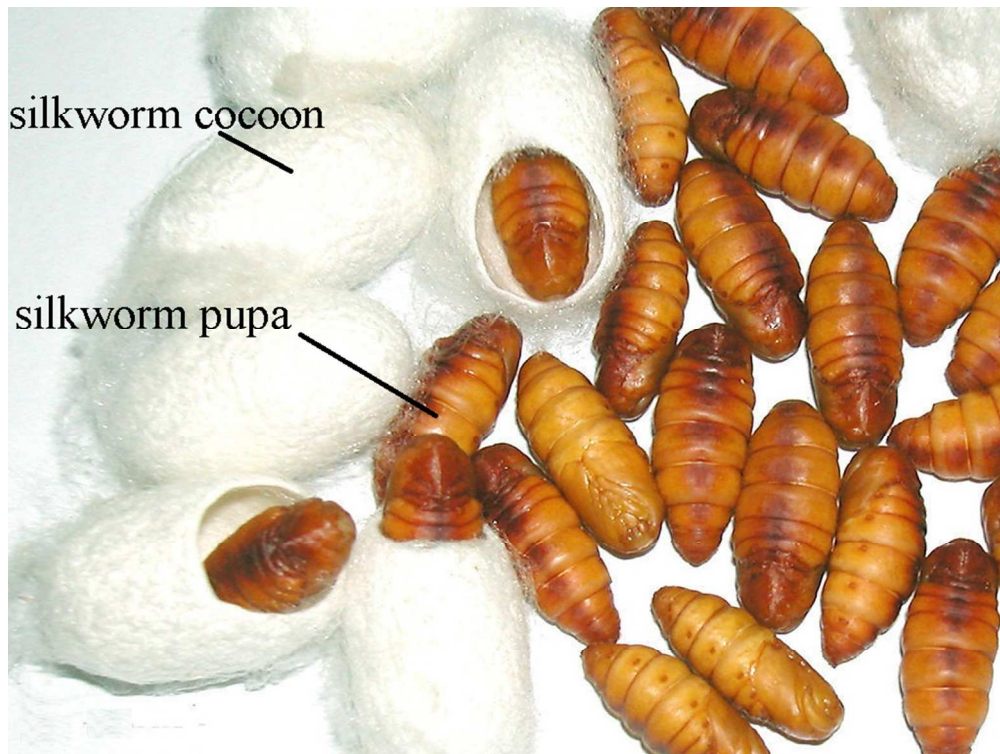


Figure1 Picture of silkworm cocoon and silkworm pupa  
361x270mm (72 x 72 DPI)

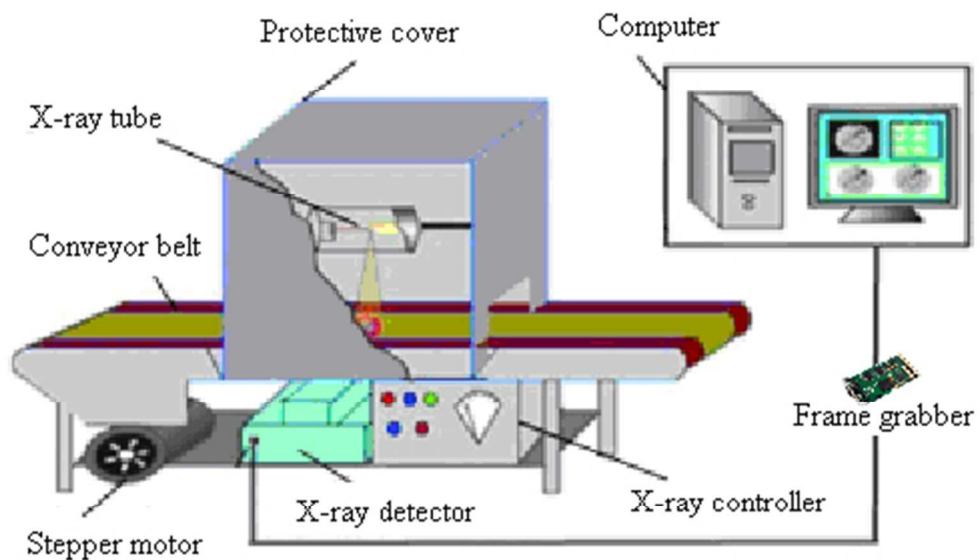


Figure2 Schematic of X-ray digital imaging system  
132x82mm (96 x 96 DPI)

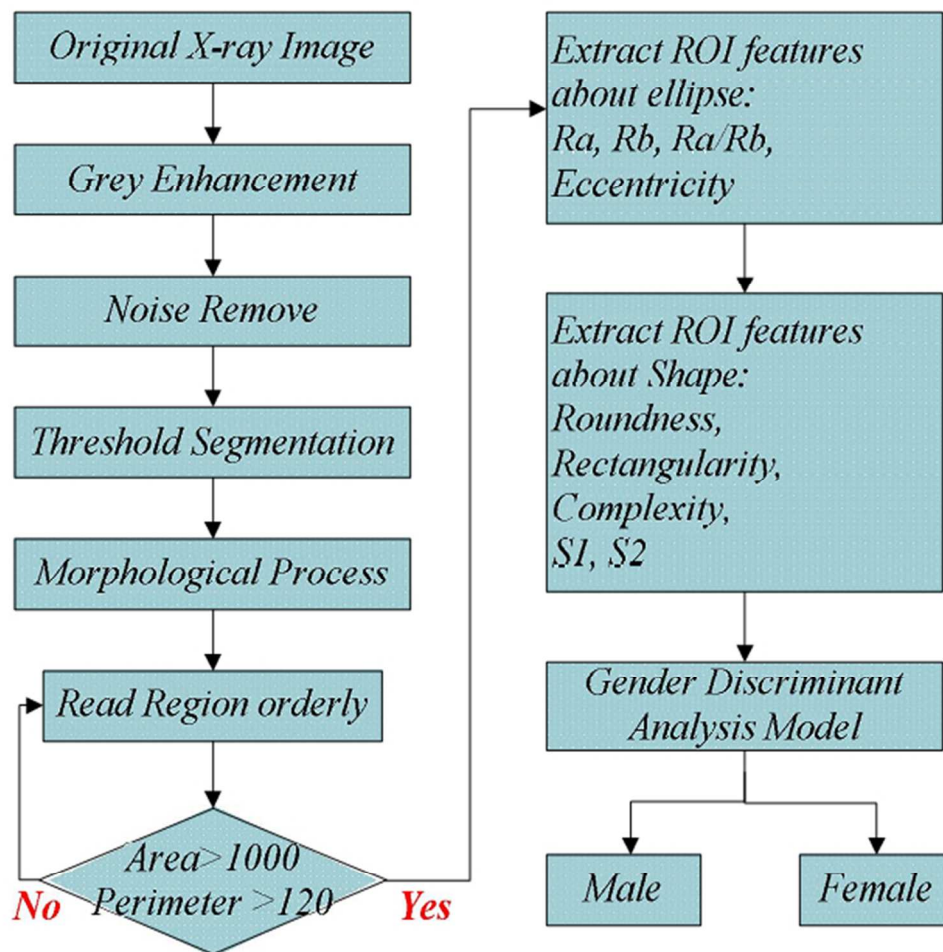


Figure3 Workflow of image processing and gender discrimination  
170x167mm (96 x 96 DPI)

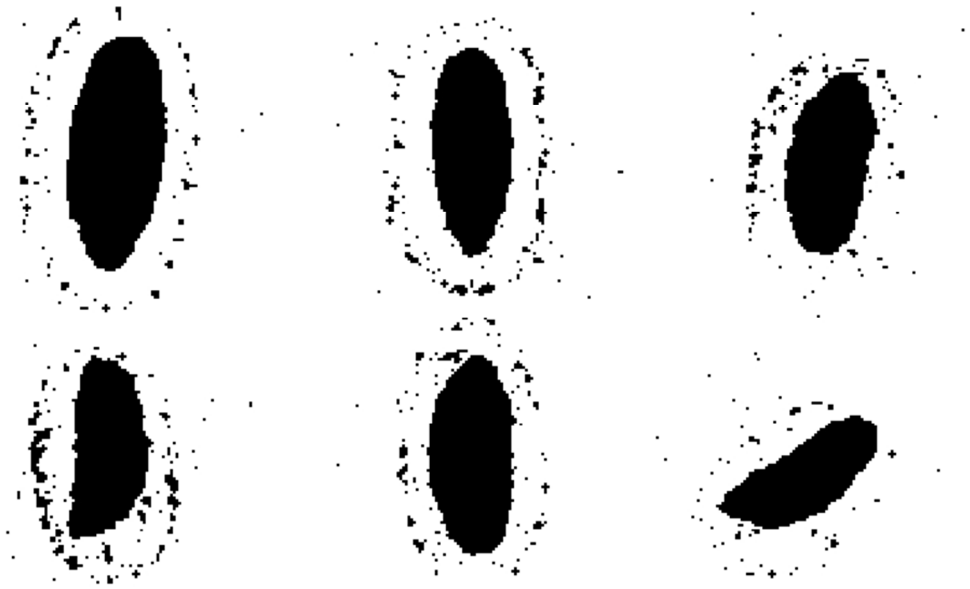


Figure4 The X-ray binary image of silkworm cocoons  
62x39mm (300 x 300 DPI)

1  
2  
3  
4  
5  
6  
7  
8  
9  
10  
11  
12  
13  
14  
15  
16  
17  
18  
19  
20  
21  
22  
23  
24  
25  
26  
27  
28  
29  
30  
31  
32  
33  
34  
35  
36  
37  
38  
39  
40  
41  
42  
43  
44  
45  
46  
47  
48  
49  
50  
51  
52  
53  
54  
55  
56  
57  
58  
59  
60

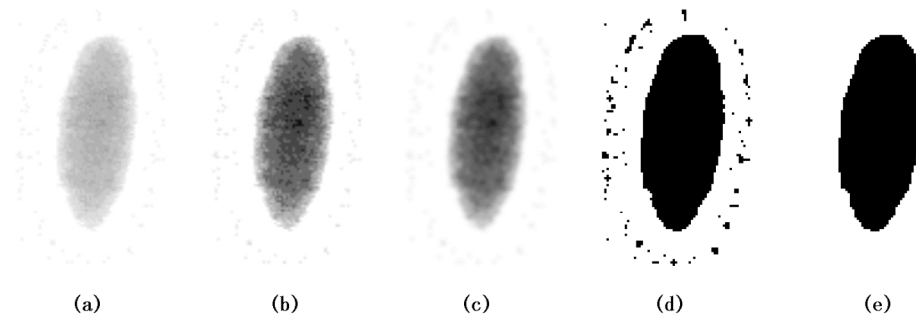


Figure5 The result of Image processes. (a) Original image; (b) Grey enhancement; (c) Gaussion filter; (d) Global threshold segmentation; (e) Opening operation output.  
148x46mm (300 x 300 DPI)

1  
2  
3  
4  
5  
6  
7  
8  
9  
10  
11  
12  
13  
14  
15  
16  
17  
18  
19  
20  
21  
22  
23  
24  
25  
26  
27  
28  
29  
30  
31  
32  
33  
34  
35  
36  
37  
38  
39  
40  
41  
42  
43  
44  
45  
46  
47  
48  
49  
50  
51  
52  
53  
54  
55  
56  
57  
58  
59  
60

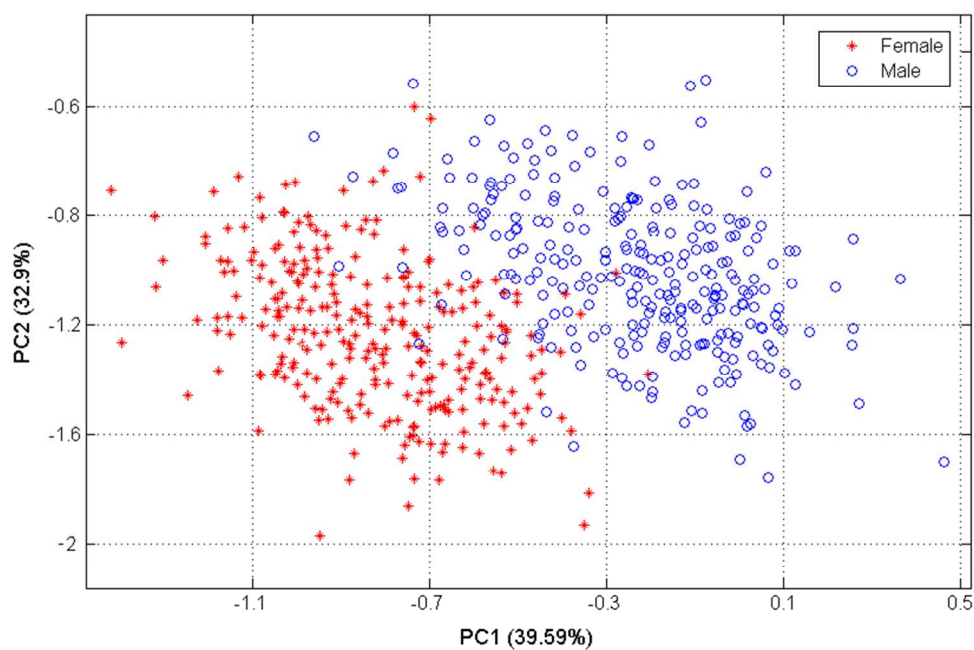


Figure6 2-D scatter plot of the gender of silkworm cocoon. PC: principal component.  
224x150mm (96 x 96 DPI)

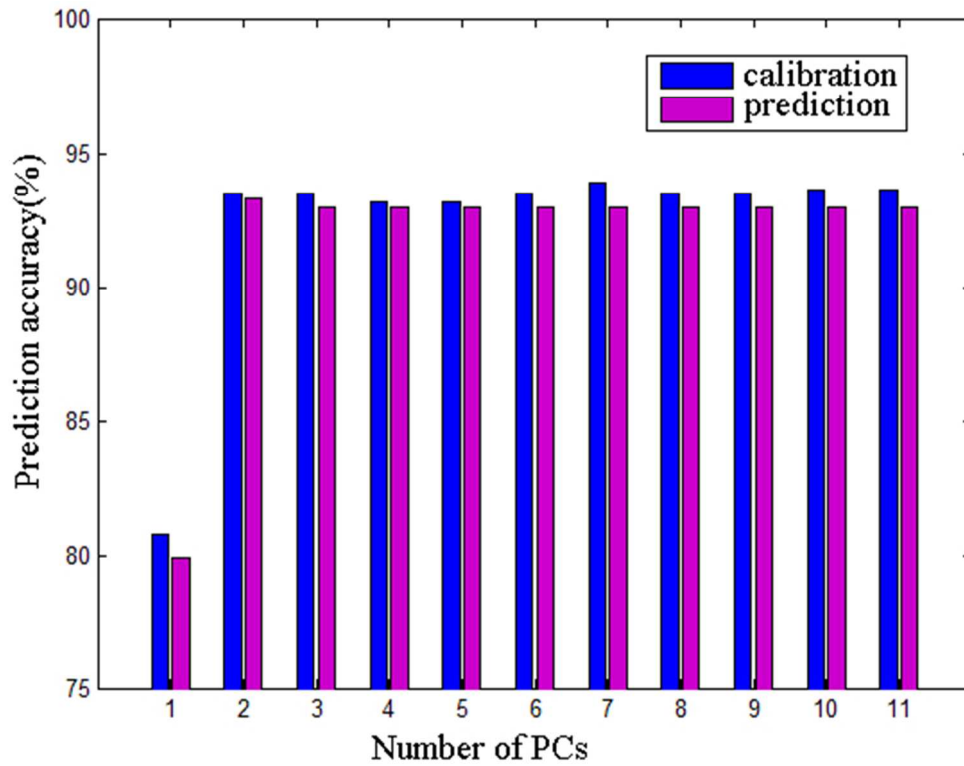


Figure7 Correct identification rates of LDA model for calibration and prediction set according to different PCs.  
147x114mm (96 x 96 DPI)

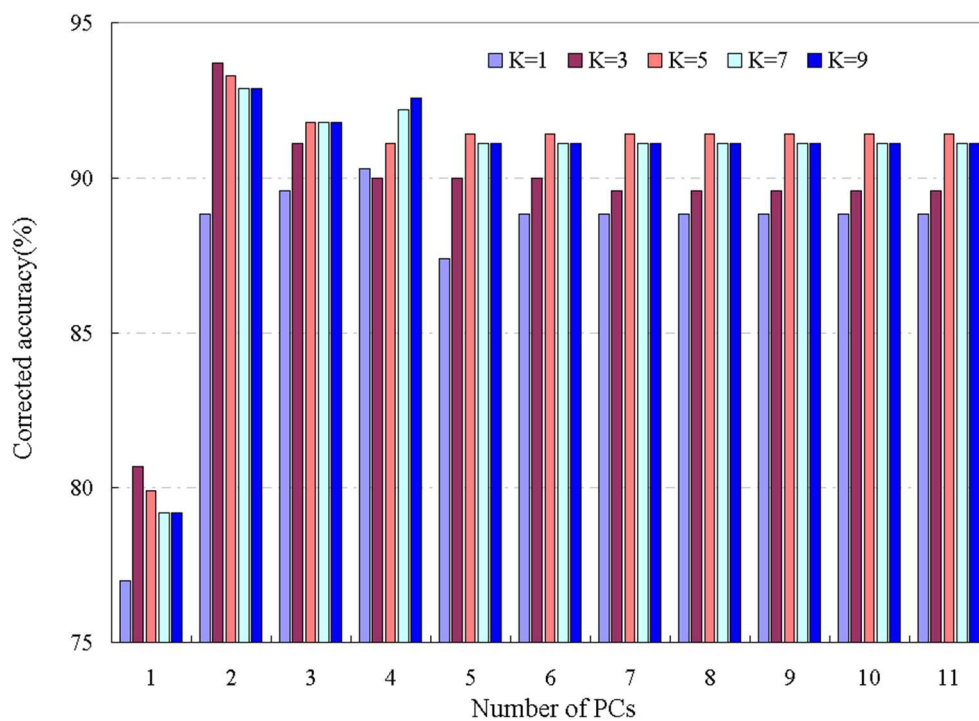


Figure8 Correct identification rate of KNN classifier for prediction set according to different PCs and K values  
251x186mm (96 x 96 DPI)

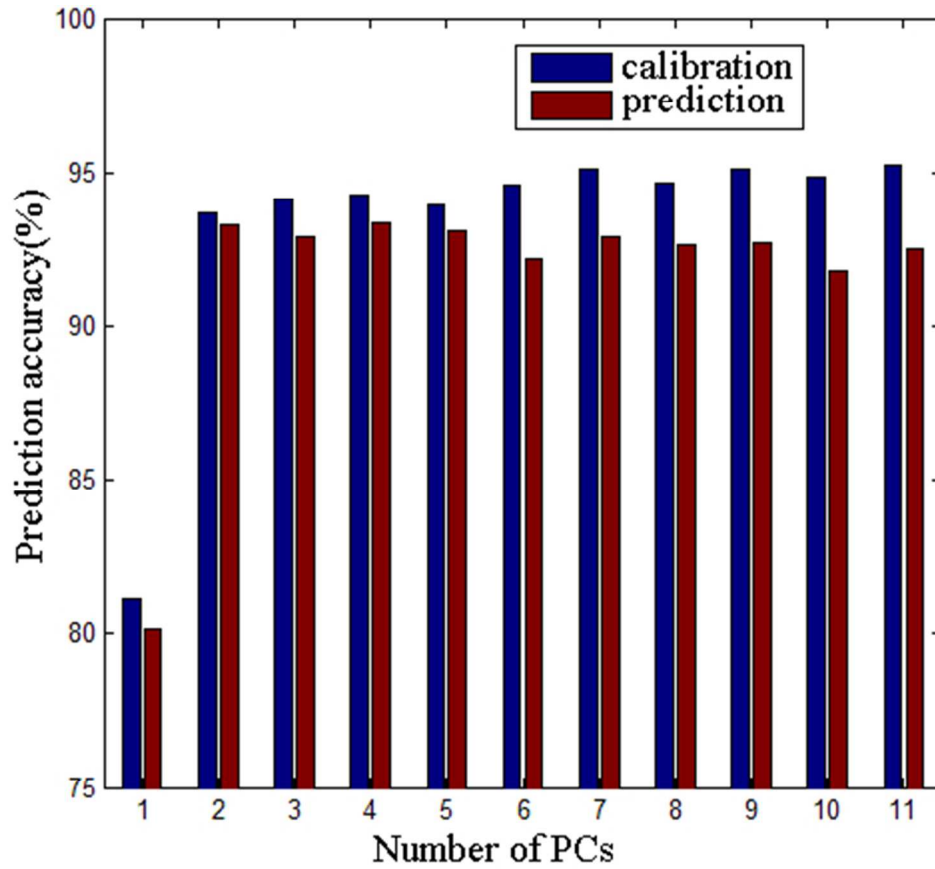


Figure9 Correct identification rate of BP-ANN model for calibration and prediction set according to different PCs.  
132x115mm (96 x 96 DPI)

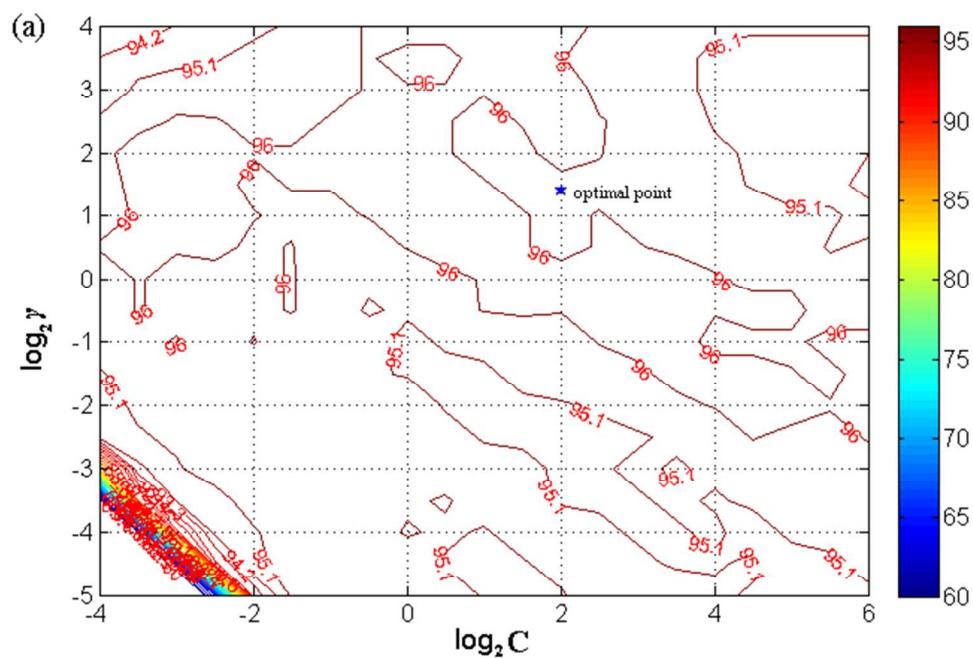


Figure10 (a) Contour plot of the optimal parameter pairs ( $C$ ,  $\gamma$ ) by cross validation based on the calibration samples; (b) Correct Identification rates of SVM classifier with different PCs for calibration and prediction set.

177x119mm (96 x 96 DPI)

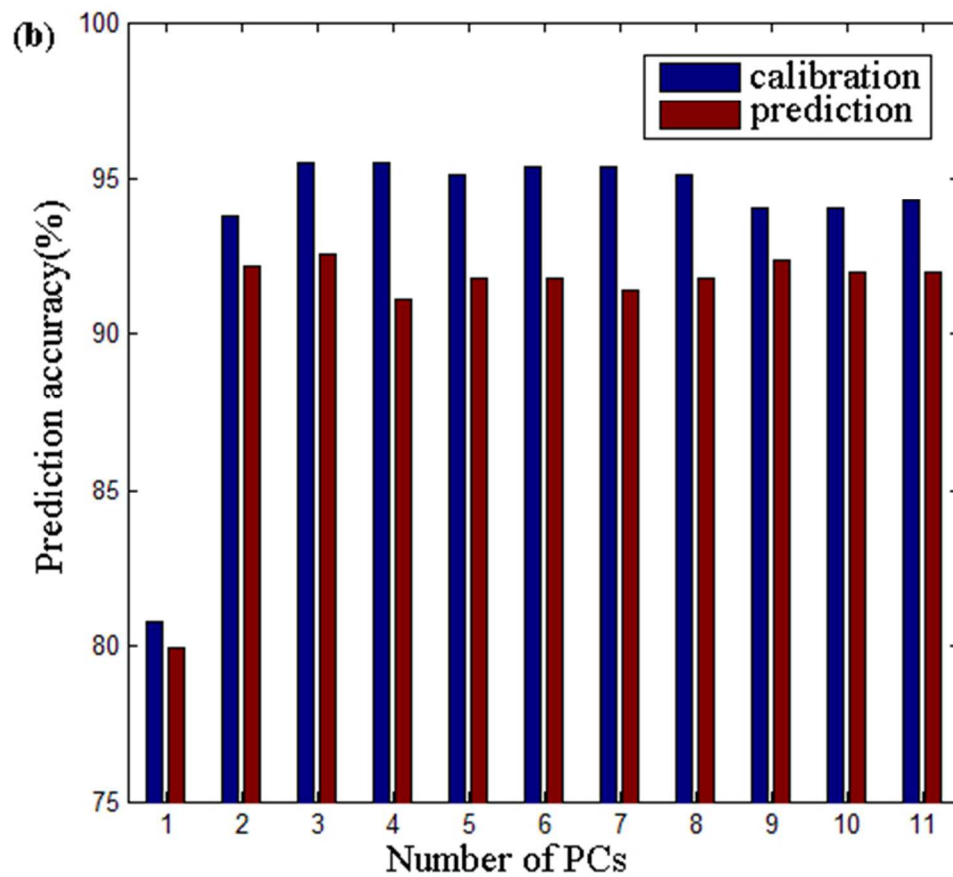


Figure10 (a) Contour plot of the optimal parameter pairs ( $C$ ,  $\gamma$ ) by cross validation based on the calibration samples; (b) Correct Identification rates of SVM classifier with different PCs for calibration and prediction set.

133x117mm (96 x 96 DPI)

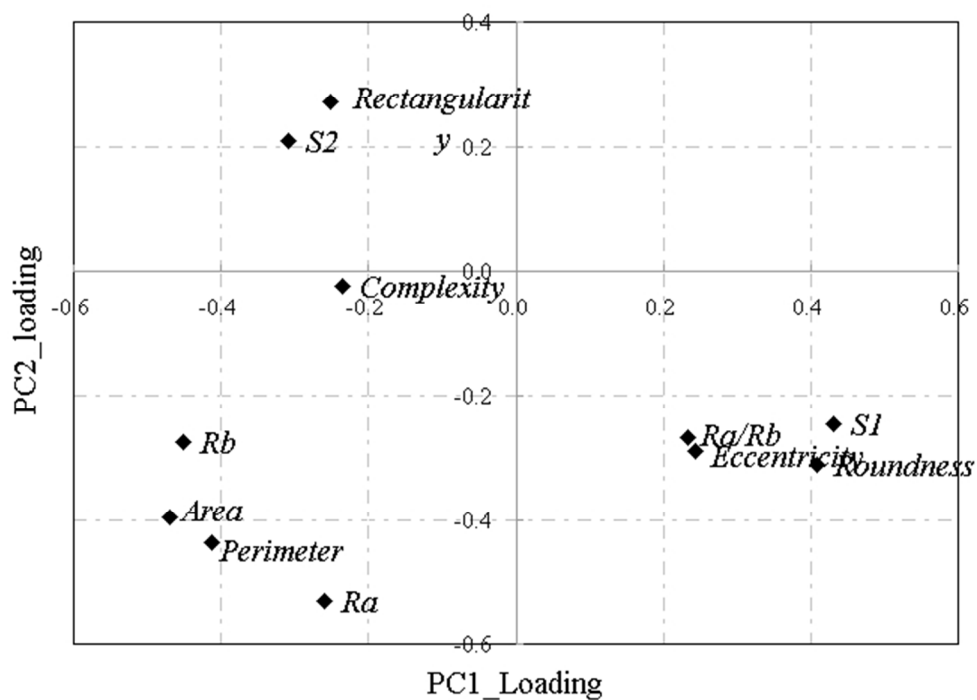


Figure 11 The loadings of top two PCs against the 11 morphological variables  
176x127mm (96 x 96 DPI)